Journal of Korean Society of
Coastal and Ocean Engineers
Vol. 8, No. 4, pp. 274~286, December 1996

Two Dimensional Flexible Body Response of Very Large Floating Structures
巨大 浮體構造物의 2次元 柔軟體 解析 및 擧動

Namseeg Hong*
洪 南 植*

Absract☐Two-dimensional flexible body analysis (hydroelasticity theory) is adopted to a very large floating structure that may be multimodule and extend in the longitudinal direction. The boundary-element method (BEM) and Green function method(GFM) are used to obtain the hydrodynamic coefficients. The structure is considered to be a flexible beam responding to waves in the vertical direction and a consistent formulation for the hydrostatic stiffness is derived. The resulting coupled equations of motion are solved directly. Two designs of the module connectors are considered: a rotationally-flexible hinge connector, and a rotationally-rigid connector. Numerical examples are presented to an integrated system of semi-submersibles. The analysis provides basic motions and section forces, which are useful to develop an understanding of the fundamental modes of displacement and force amplitudes for which multi-module VLFSs must be designed. The results show that while the hinge connectors result in greater motion, the rigid connectors increase substantially the sectional moments.

要 旨 : 2차원 유연체해석 이론(수탄성 이론)을 여러개의 단위체 연결로 이루어진 거대 부체구조물의 해석에 적용하였다. 동수역학적 계수를 구하기 위해 경계요소법과 그린함수법이 사용되었으며 부체자체는 연직방향으로 파랑에 반응하는 연체보로 정수역학적 탄성계수에 대한 운동을 고려하여 운동방정식이 유도된다. 두가지 다른 형식의 연결, 즉 회전강성을 가진 것과 강성을 무시한 핀 형식의 연결요소가 고려되며 반잠수한 부체에 대해 해석결과가 제시된다. 해석결과는 거대 부체구조물의 설계에 필요한 변위와 내력에 관한 개념을 제시한다. 또한 수치해석 결과에 따르면 부체의 움직임은 핀연결이 강성체 연결보다 더 크며 부체의 내력휨 응력은 강성체 연결에서 훨씬 더 크게 증가하였다.

1. INTRODUCTION

Very Large Floating Structures (VLFSs) have been proposed for a number of applications: airports, runways, military bases, wave power generation, deep ocean mining, industrial facilities, and entire floating cities(Seidl, 1973; St. Denis, 1974). Nearshore applications are frequently motivated by a desire to extend the available surface area near the centers of coastal urban areas. A typical example is the floating airport, such as the one considered for the city of San Diego (USD, 1990) as an alternative to a more distant inland airport. Open ocean applications would provide a stable platform for functions which are best carried out in geographic areas far from any land mass.

VLFSs will be of a scale never before constructed in a marine environment. Perhaps the largest floating structures constructed to date are floating bridges, such as the inland Hood Canal bridge, which was approximately 2000 m long but only 15m wide (Hartz, 1981). A floating airport, on the other hand, would be at least as long, several hundred meters wide, and located in an

*삼성물산 건설부문 토목 ENG.팀 (Civil Eng. Team, Engineering & Construction Group, Samsung Corporation, Seoul 135-080, Korea)

exposed ocean environment. However, the basic technology required for their construction may be available, because it is likely that a large class of VLFSs will consist of multiple, conventional-sized modules connected together. Due to the size and possible multimodule configuration, the design of such a structure and the analysis of its behavior in waves may be different from those of existing floating structures. The primary concerns are those of wave loading and response of a VLFS in regular waves. In this paper, a method is presented for predicting the loading and response of a VLFS in regular waves.

The system to be analyzed has the configuration shown in Fig. 1. The platform is composed of several modules connected in longitude direction. Each module consists in a deck, 100 by 100 m in extent, supported by a column near each corner; each longitudinal pair of columns is, in turn, supported by a pontoon; the pontoons and the decks are mutually connected in vertical shear and bending. The system is not moored, but is considered to remain stationary in location.

The system can be modeled in two ways. In the first model, the longitudinal sequence of modules is considered as a single beam having varying shear and flexural rigidities. With such a model, the response of the system to wave excitation is analyzed by a two-dimensional hydroelastic theory that considers mutual interaction among inertia, hydrodynamic and elastic forces(Heller and Abramson, 1959). In the second model, the modules are considered to be rigid, that is undeformable by the wave loading; they respond to waves as a sequence of rigid modules flexibly connected (RMFC). Such a model is valid only if the deformation, that is, the vibrations, of the modules under wave loading are so small that they do not affect such loading. Once the wave loading and oscillatory response of the system have been determined, each module can then be considered to be an isolated body for the calculation of the elastic stresses in flexure and shear. Both methods are employed herein and their relative efficiency is discussed.

The boundary-element method (BEM) and Green function method (GFM) are used to obtain the hydrodynamic coefficients. Numerical results are given for illustration.

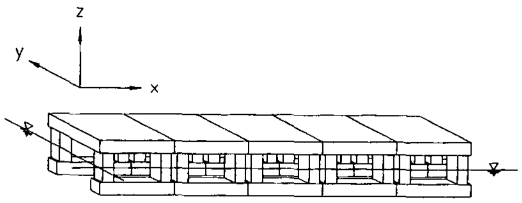

Fig. 1. Three-dimensional view of VLFS.

2. HYDRODYNAMIC FORCES

Strip theory has proved to be a good approach for estimating the fluid action on a slender body (Bishop and Price, 1979; Lee *et al.*, 1971; Gerritsma and Beukelman, 1964). The theory is based on the assumption that the disturbance of the fluid caused by the motion of the body does not generate the secondary fluid motion. This assumption gives a reasonable approximation if $L>>B$ and $L>>D$, where L, B and D are the length, beam and draft of the structure, respectively. According to the revised strip theory of Flokstra(1974), the vertical force Z, in the absence of forward speed, is given by

$$Z(x,t)=-\frac{\partial}{\partial t}\left\{\left[m(x)+\frac{i}{\omega}N(x)\right]\frac{\partial}{\partial t}\left[w(x,t)-\bar{\zeta}(x,t)\right]\right\}$$
$$-\rho g B(x)\left[w(x,t)-\bar{\zeta}(x,t)\right] \tag{1}$$

where $\bar{\zeta}(x,t)$ is the wave elevation modified for the Smith effect, that is

$$\bar{\zeta}(x,t)=S_m(x)\zeta(x,0,t)$$
$$S_m(x)=1-k\int_{-D}^{0}\exp(kz)dz \tag{2}$$

where $\zeta(x, y, t)$ is the actual wave elevation, and $k=\omega^2/g=2\pi/\lambda$ is the wave number. The integral is over the wetted half contour $C(x)$ (see Fig. 2). Here, only the case of head seas, that is, x=180 deg, is considered.

The hydrodynamic mass and damping coefficients in heave, $m(x)$ and $N(x)$, defined in (1), are obtained by

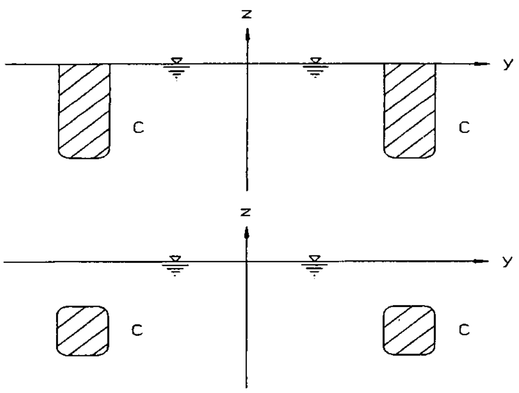

Fig. 2. Immersed contours of two sections: one with columns and pontoons.

solving the two-dimensional radiation problem of an infinitely long cylinder, whose cross-sectional contour is $C(x)$, oscillating with unit amplitude and frequency ω on the water surface. These coefficients are given by

$$m(x) = -\rho R\left\{\int_{C(x)} \phi(y,z)n_3\,dC\right\},$$

$$N(x) = \omega\rho I\left\{\int_{C(x)} \phi(y,z)n_3\,dC\right\} \quad (3)$$

where n_3 is the component of the unit normal vector of the contour $C(x)$ in the z-direction, and R and I denote the real and imaginary parts of the integrals, respectively. The velocity potential ϕ must satisfy the following equations:

$$\frac{\partial^2\phi}{\partial y^2} + \frac{\partial^2\phi}{\partial z^2} = 0 \text{ (within the fluid domain)} \quad (4a)$$

$$-\omega^2\phi + g\frac{\partial\phi}{\partial z} = 0 \text{ (on } z=0\text{)} \quad (4b)$$

$$\frac{\partial\phi}{\partial n} = n_3 \text{ (on } C\text{)} \quad (4c)$$

$$\lim_{z\to\mp\infty}\frac{\partial\phi}{\partial z} = 0 \text{ (on the sea floor)} \quad (4d)$$

In addition, the two-dimensional radiation condition needs to be satisfied at infinite distances from the contour C. This condition is stated by

$$\lim_{y\to\mp\infty}\left(\frac{\partial\phi}{\partial y} \mp ik\phi\right) = 0 \text{ (on } C_{R+} \cup C_{R-}\text{)} \quad (5)$$

It guarantees the uniqueness of the solution. Physically speaking, it ensures that the generated waves radiate outward, and die out infinitely far from the source of the disturbance.

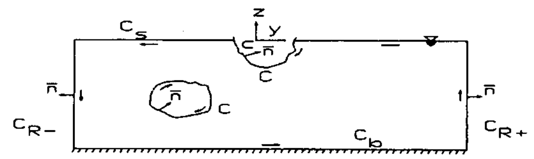

Fig. 3. Sketch for boundary integral formulation.

In this study, both the BEM and the GFM are adopted to solve ϕ. Specially for the case of hull structures, these two methods are shown to be efficient.

2.1 Boundary-Element Method

The boundary element method (Brebbia, 1978; Andres, 1986) is applied here to obtain the hydrodynamic coefficients. The two-dimensional radiation problem can be solved by making use of Green's second identity. It results that

$$\int_n (\phi\nabla^2 G - G\nabla^2\phi)\,d\Omega = \int_{C_r}\left(\phi\frac{\partial G}{\partial n} - G\frac{\partial\phi}{\partial n}\right)dC \quad (6)$$

where ϕ and G are functions that have continuous first derivatives in the closed regular region Ω, which is bounded by the curve, C_T, and where $\partial/\partial n$ is the derivative in the direction of the unit normal vector; see Fig. 3.

Upon selecting the Green function G as the solution corresponding to a point source, the above equation can be reduced to an integral equation over the whole boundary C_T. For a two-dimensional problem, the fundamental solution of Laplace's equation is

$$G(P,Q) = \frac{1}{2\pi}\ln\left(\frac{1}{\gamma}\right) \quad (7)$$

where

$$\gamma = \sqrt{(y-\xi)^2(z-\zeta)^2},\ P = P(y,z),\ Q = Q(\xi,\zeta)$$

In this case $G(P, Q)$ satisfies Laplace's equation everywhere except at Q, where the point source is located. Upon combining the conditions in equations (4b), (4c), (4d), (5) and substituting $G(P, Q)$ into (6), the following boundary integral equation is obtained:

$$\frac{1}{2}\phi = \int_C \left[\phi \frac{\partial}{\partial n}\left(\ln\frac{1}{\gamma}\right) - \ln\left(\frac{1}{\gamma}\right) n_3 \right] dC$$

$$+ \int_{C_{R+} \cup C_{R-}} \left[\phi \frac{\partial}{\partial n}\left(\ln\frac{1}{\gamma}\right) \mp ik \ln\left(\frac{1}{\gamma}\right) \right] dC$$

$$+ \int_{C_s} \left[\phi \frac{\partial}{\partial n}\left(\frac{1}{\gamma}\right) - \frac{\omega^2}{g} \ln\left(\frac{1}{\gamma}\right) \right] dC$$

$$+ \int_{C_b} \phi \frac{\partial}{\partial n}\left(\ln\frac{1}{\gamma}\right) dC \tag{8}$$

where C, C_{R+}, C_{R-}, C_S, C_b are the boundaries of the body, and at far right, far left, free surface, and bottom, respectively.

To solve this integral equation, the boundary of the whole domain is subdivided into elements. The values of $G(P, Q)$ and $\partial G/\partial n$ at the center of each element are then derived and introduced in (8). A matrix of linear equations is thus obtained. The node value of the potential is calculated from the resulting system of linear algebraic equations.

2.2 Green Function Method

The Green function method (Frank, 1967; Garrison, 1984) is applied to estimate the added-mass and damping coefficients. This method requires less computational time but a greater mathematical treatment than does the alternative BEM. The two-dimensional GFM, which was first applied by Frank, is recalled for convenience.

The solution of the radiation problem is assumed to be represented by a distribution of singularities over the immersed sectional contour of the structure (Kellog, 1929):

$$\phi(P) = -\frac{1}{2\pi} \int_C o-(Q) G(P,Q)\, dC \tag{9}$$

where $P(y, z)$ is the field point, $Q(\xi, \eta)$ is the source point, $o-(Q)$ is source density, C is the immersed contour of the structure, and $G(P, Q)$ is the Green function.

The Green function corresponding to a source of unit strength located below a free surface is given by

$$G(P,Q) = \ln(\gamma) + G^*(P,Q) \tag{10}$$

where $\gamma = \sqrt{(y-\xi)^2 - (z-\zeta)^2}$, and $G^*(P, Q)$ is a harmonic function.

According to the radiation problem stated earlier, it is required that $G(P, Q)$ satisfy the boundary-value problem as follows:

Governing equation: $\dfrac{\partial^2 G}{\partial y^2} + \dfrac{\partial^2 G}{\partial z^2} = \delta(P,Q)$

Free-surface condition: $\dfrac{\partial G}{\partial z} - kG = 0$

Bottom condition: $\lim_{z \to -\infty} \nabla G = 0$

Sommerfeld condition: $\lim_{y \to \mp\infty} \left(\dfrac{\partial G}{\partial y} \pm ikG \right) = 0$ (11)

The Green function that satisfies the equations in (11) has been solved to yield (Wehausen and Laitone, 1960; Mei, 1989)

$$G(P,Q) = \ln(\gamma) - \ln(\gamma_1) + 2P.V. \int_0^\infty \exp(m(z+\zeta)) \frac{\cos(m(y-\xi))}{m-k}\, dm - i \exp (k(z+\zeta) \cos(k(y-\xi)) \tag{12}$$

and $P.V.$ denotes the principal value integral. A detailed derivation of (12) is given, for example, by Mei (1989). When the kinematic boundary condition given by (4c) is imposed on (9), it follows that

$$\frac{\partial \phi(P)}{\partial n} = n_3 = \frac{1}{2}\sigma(P) + \frac{1}{2\pi} \int_C \sigma(Q) \frac{\partial G(P,Q)}{\partial n}\, dC \tag{13}$$

This equation is used to determine the source density $\sigma(Q)$.

It is assumed that the contour of the floating structure C can be approximated by N straight-line segments, each of which is denoted by C_j, j=1, 2,..., N. Thus, (9) and (13) can be written as

$$\phi(P_n) = \frac{1}{2\pi} \sum_{\substack{j=1 \\ j \neq n}}^{N} \int_{C_j} \sigma_j G(P_n, Q_j)\, dC \tag{14}$$

$$\frac{\partial\phi(P_n)}{\partial n} = n_3(P_n) = \frac{1}{2}\sigma_n(P_n) + \frac{1}{2\pi}\sum_{\substack{i=1\\ j\neq n}}^{N}\int_{C_i}\sigma_j(Q_j)\frac{\partial G(P_n,Q_j)}{\partial n}dC \tag{15}$$

for n=1, 2,..., N. Clearly, the above equations will be accurate as long as the segment size is small in comparison with the wavelength of the waves generated by the motion of the body.

Once the solution to (15) for the source strength σ_j has been obtained, the potential at any point on the immersed contour C follows immediately. Hence, the dynamic pressure on the immersed surface of the body can be determined form of Euler's integral when the motion is harmonic, that is, when

$$p = i\rho\omega\phi \tag{16}$$

As a result, the expression for the hydrodynamic heaving force on the structure is

$$F = \exp(-i\omega t)\int_C pn_e\, dc = \exp(-i\omega t)i\rho\omega\int_C \phi n_3 dC$$
$$= \exp(-i\omega t)i\rho\omega\int_C \phi\frac{\partial\phi}{\partial n}dC \tag{17}$$

The hydrodynamic force can also be expressed as

$$F = \frac{\partial u}{\partial t}m - uN \tag{18}$$

where u=1 · exp(-$i\omega$t). Combining (17) and (18), we have

$$\rho\int_C \phi\frac{\partial\phi}{\partial n}dC = m + \frac{i}{\omega}N \tag{19}$$

which is consistent with (3) when ϕ is a complex function. The complex form of ϕ is necessary in order that the radiation condition be satisfied. The exciting force is given by (1), that is, the Haskind-Hanaoka relationship, written in terms of radiation, and Froude-Krylov forces.

It should be noted that for some discrete 'irregular' frequencies the Green function method fails to give a solution. This occurs when the fluid field extends into an interior region which is also bounded in part by a free surface. John(1950) shows that an irregular-frequency phenomenon occurs when the adjacent interior potential problem has a modal frequency which coincides with the frequency of oscillation.

The results of the two cases for two pontoons and two pontoons with columns are shown in Fig. 4. These results are obtained by the BEM and the GFM. Fig. 4 shows plots of $\bar{m} = m(x)/(\partial\forall)$ and $\bar{N} = N(x)/(\rho\forall\sqrt{g/L})$ where ρ is the density of fluid, $\forall$ is the volume of the body immersed, g is the gravitational acceleration and L is a scale length. The agreement between the BEM and GFM results are, in general, satisfactory, aside from the apparent lack of irregular frequencies in GFM predictions.

3. STRUCTURAL MODEL

The configuration of a single module of VLFS is shown in Fig. 5. Simplification reduces the system to be analyzed from a sequence of modules to a connected sequence of column-carrying pontoons, and the problem of analysis becomes two-dimensional one. If only the vertical motions and distortions are taken into account, and the coordinate system shown in Fig. 6 is introduced, the strutural dynamic equations of motion, according to Timoshenko's beam theory, are

$$\mu\frac{\partial^2\omega}{\partial t^2} - \frac{\partial}{\partial x}\left[KAG\left(\gamma + \frac{\partial\gamma}{\partial t}\right)\right] = Z,$$

$$J\frac{\partial^2\theta}{\partial t^2} - \frac{\partial}{\partial x}\left[EI\left(\frac{\partial\theta}{\partial x} + \beta\frac{\partial^2\theta}{\partial x\partial t}\right)\right] - KAG\left(\gamma + \alpha\frac{\partial\gamma}{\partial t}\right) = 0 \tag{20}$$

where μ, J, EI and KAG are, respectively, the mass per unit length, the moment of inertia in pitch per unit length, the flexural rigidity in vertical bending, and the equivalent shearing rigidity of the beam, all being functions of the x-coordinate, while α and β are, respectively, the structural damping coefficients in shear and bending. Z is the external time-varying vertical force, ω, θ, and γ are the vertical deflection, the angle of rotation of the cross section about the transverse axis

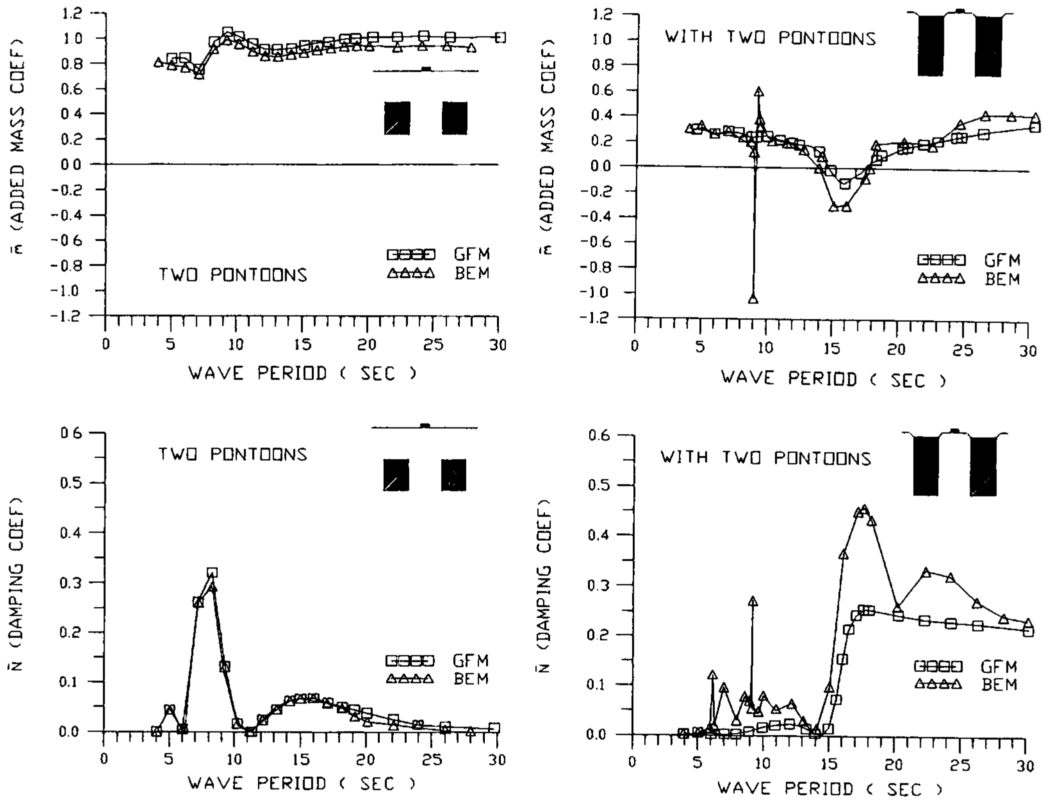

Fig. 4. Hydrodynamic coefficients in heave direction.

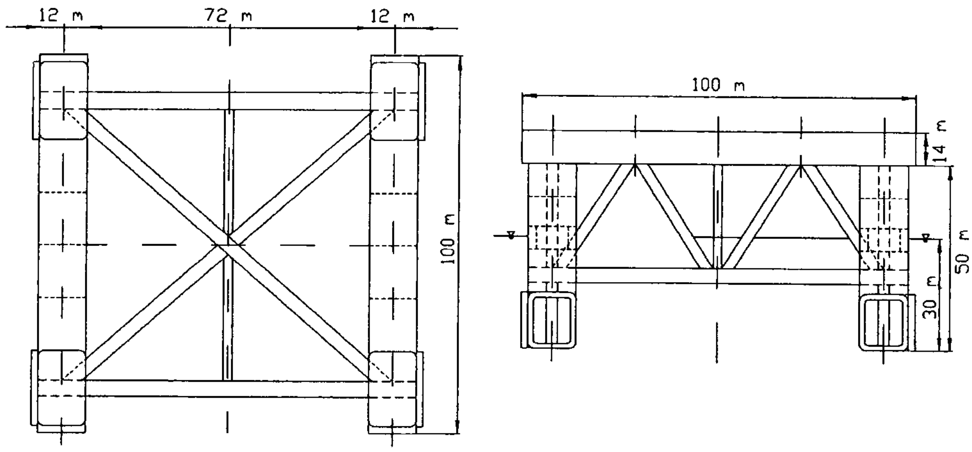

Fig. 5. Configuration of a single module.

due to bending, and the shear strain, respectively; they are all functions of x and t and satisfy the following relationship (Timoshenko *et al.*, 1974).

$$\frac{\partial \omega}{\partial x} = \theta + \gamma \tag{21}$$

When the boundary conditions at the two free ends are imposed, and α, β and Z are set equal to zero, the solution of the equations yields the undamped natural frequencies ω_j and the principal modes of free vibration ($\omega_j(x)$, $\theta_j(x)$, $\gamma_j(x)$, J=2, 3,....). Here the first distortion

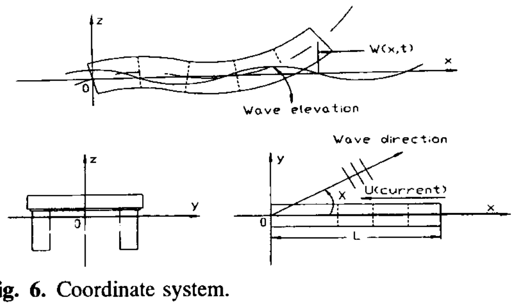

Fig. 6. Coordinate system.

mode is denoted by j=2, for the reason that it has two nodes. And, j=0 and 1 are used to denote the two vertical rigid body modes, namely heave (j=0) and pitch (j=1).

The forced response of a structure can be expressed by modal superposition (Rayleigh, 1970) as

$$\begin{aligned} \omega(x,t) &= \sum_{j=0}^{n} \omega_j(x) P_j(t) \\ \theta(x,t) &= \sum_{j=0}^{n} \theta_j(x) P_j(t) \\ \gamma(x,t) &= \sum_{j=0}^{n} \gamma_j(x) P_j(x) \end{aligned} \tag{22}$$

where $P_j(t)$=0, 1, 2,...., n, are the principal coordinates. The summation in the expressions can usually be restricted to the lowest n principal modes (n=0, 1, 2, 3, 4, 5 are used in this study). The structural equations of motion (20), can be converted to the following form to be solved for the principal coordinates:

$$[a]\left\{\frac{\partial^2 P}{\partial t^2}\right\} + [b]\left\{\frac{\partial P}{\partial t}\right\} + [c][P] = [F] \tag{23}$$

where $[a]$, $[c]$ and $[F]$ are the matrices of generalized mass, stiffness and external force, respectively. The elements of these matrices are

$$\begin{aligned} a_{ij} &= \int_0^L (\mu\, \omega_i\, \omega_j + J\, \theta_i\, \theta_j)\, dx \\ c_{ij} &= \delta_{ij}\, \omega_i^2\, a_{ij} = \int_0^L \left(EI \frac{\partial \theta_i}{\partial t} \frac{\partial \theta_j}{\partial x} + KAG\, \gamma_i\, \gamma_j \right) dx \\ F_i &= \int_0^L Z_\omega\, dx \end{aligned} \tag{24}$$

where i, j=0, 1,..., n. Here δ_{ij} is the Kronecker delta function. All the fluid actions are now contained in the external force term Z, and are, evidently, motion and deflection dependent. The elements of the generalized structural damping matrix are given by

$$b_{ij} = \int_0^L \left(\alpha KAG\, \gamma_i\, \gamma_j + \beta EI \frac{\partial \theta_i}{\partial x} \frac{\partial \theta_j}{\partial x} \right) dx \tag{25}$$

Equation (23) is to be solved together with the analysis of coupled hydrodynamic forces. Once the principal coordinates are known, the calculation of motions and distortions is a straightforward application of (22). Furthermore, the bending moment $M(x, t)$ and the shear force $V(x, t)=KAG\gamma(x, t)$ at any cross section of the structure can be obtained from the corresponding principal modes $M_j(x)$ and $V_j(x)$ as:

$$M(x,t) = \sum_{j=2}^{n} M_j(x) P_j(t),\ V(x,t) = \sum_{j=2}^{n} V_j(x) P_j(t) \tag{26}$$

4. ASSEMBLED GOVERNING EQUATIONS OF MOTIONS

The equation (23) can be modified by including fludic effect as

$$\begin{aligned} &([a]+[A])\left\{\frac{\partial^2 P}{\partial t^2}\right\} + ([b]+[B])\left\{\frac{\partial P}{\partial t}\right\} \\ &+ ([c]+[C])\{p\} = \{E\ (t)\} \end{aligned} \tag{27}$$

The matrices $[A]$, $[B]$ and $[C]$ contain the generalized hydrodynamic added-mass coefficients A_{ij}, damping coefficients B_{ij}, and hydrostatic restoring coefficients C_{ij} given by the following expressions:

$$A_{ij} = \int_0^L m(x) w_i(x) w_j(x)\, dx \tag{28}$$

$$B_{ij} = \int_0^L N(x) w_i(x) w_j(x)\, dx \tag{29}$$

$$C_{ij} = pg \int_0^L B(x) w_i(x) w_j(x)\, dx \tag{30}$$

The wave-excitation forces in regular waves, E_i, are now given by

$$\begin{aligned} E_i(t) &= \int_0^L S_m(x) \exp(-i(kx+\omega t))\, [-\omega^2 m(x) - i\omega N(x) \\ &+ \rho g B(x)]\, w_i(x) dx = E_i \exp(-i\omega t) \end{aligned} \tag{31}$$

The time harmonic response of the structure encountering regular waves is such that

$$[p] \equiv (\{[c]+[C]\} - \omega^2\{[a]+[A]\} - i\omega\{[b]+[B]\})^{-1}\{E\} \tag{32}$$

5. PRACTICAL APPLICATION OF THE HINGE CONNECTOR

In practical applications, a VLFS will most likely consist of multiple modules linked with especially designed intermodule connectors. Because the connectors' bending stiffness is likely to be much less than that of the modules, the structure can be represented approximately by a series of rigid modules connected by hinge connectors. In this case, since only vertical motions are considered, each module has only two degrees of freedom, that is, heave and pitch. The equation of motion for the structure is then

$$[a]\left\{\frac{\partial^2 Y_n}{\partial t^2}\right\} + [b]\left\{\frac{\partial Y_n}{\partial t}\right\} + [c]\{Y_n\} = \{Z_T\} \tag{33}$$

where $[a]$, $[b]$, and $[c]$ are the mass, structural damping, and stiffness matrices of the dry structure, respectively; $\{Y_n\}$ is the nodal displacement vector; and $\{Z_T\}$ is a vector of all hydrodynamic forces, including diffraction and radiation forces. A further simplification results if it is assumed that there is no hydrodynamic interaction between modules, in which case the hydrodynamic added mass and damping of a single rigid module can be used for each module of a VLFS. The hydrodynamic added-mass matrix $[A]$ and damping matrix $[B]$ are assembled in a straightforward manner and added to the structure matrices. Similarly, the hydrostatic stiffness matrix $[c]$ is assembled. The equations of motion then can be written as

$$[a+A]\left\{\frac{\partial Y_n}{\partial t^2}\right\} + [b+B]\left\{\frac{\partial Y_n}{\partial t}\right\} + [c+C]\{Y_n\} = \{Z\} \tag{34}$$

where $[Z]$ is the exciting force.

It is assumed here that the connectors allow only relative rotation between modules (that is, no relative longitudinal or vertical displacement). Thus, there are

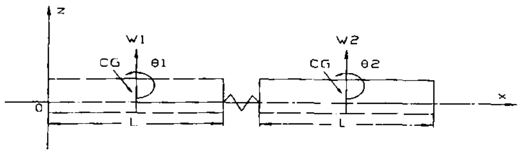

Fig. 7. Rigid modules with flexible connectors (two-module case).

only n+1 independent displacements, where n is the number of modules, as the displacements in $\{Y_n\}$ are subject to the constraints

$$w_i + \frac{L}{2}\theta_i = w_{i+1} - \frac{L}{2}\theta_{i+1} \tag{35}$$

These constraints can be used to develop the equations of motion from (34) as follows. If consideration is lim- ited to the two-module VLFS shown in Fig. 7, the kinematically independent displacements are taken as $[Y_d]=\{\theta_1, w_1, w_2\}^T$. From Eq. (35), one obtains $\{Y_n\}=[R]\{Y_d\}$, where

$$[R] = \begin{bmatrix} 0 & 1 & 0 \\ 1 & 0 & 0 \\ 0 & 0 & 1 \\ -1 & -2/L & 2/L \end{bmatrix} \tag{36}$$

The equations of motion then become

$$[R]^T[a+A\,I\,R]\left\{\frac{\partial^2 U_n}{\partial t^2}\right\} + [R]^T[b+B\,I\,R]\left\{\frac{\partial U_n}{\partial t}\right\} + [R]^T[c+C\,I\,R]\{U_n\} = [R]^T\{Z\} \tag{37}$$

Equation (37) is valid for any number of modules so long as the transformation matrix $[R]$ is defined properly.

6. NUMERICAL APPLICATION AND RESULTS

The structure to be analyzed here is a five-module floating structure of which each module consists in a deck 100 by 100 m shown in Figs. 1 and 5.

The stiffness of the modules is much greater than that of the connector. As mentioned before, two methods are used to solve this problem. In the first, the structure is treated as a slender continuous beam whose stiffness between the modules is very much less than that along the modules. The numerical results for the motion response of such a structure in regular head seas of unit amplitude are obtained based on the theory presented. In the second method, the motion response of the rigid modules, connected with hinges, is calculated. The results obtained by these two methods are compared below.

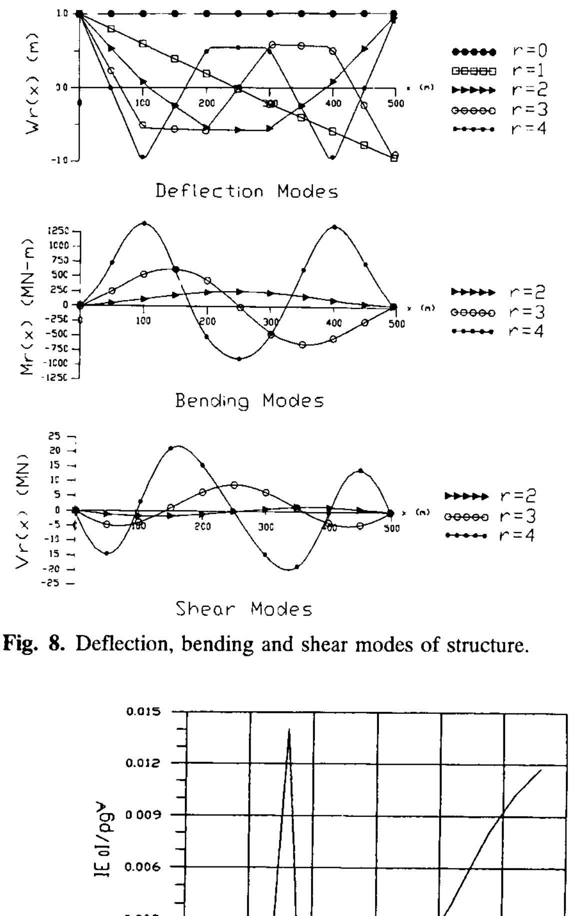

Fig. 8. Deflection, bending and shear modes of structure.

6.1 The Flexible Rigid Connector Model

The modal shapes, Fig. 8, illustrate the characteristics of such a structure consisting of almost rigid bodies joined by very flexible connectors.

For the calculation of the hydrodynamic coefficients, the BEM and the GFM give results in fair agreement (see Fig. 4). The generalized wave force is then obtained from (31). The generalized wave exciting force is shown in Fig. 9.

Fig. 10 shows the variation of the dimensionless amplitudes of the principal coordinates. The heave and pitch motions dominate the response at the very large wave periods. It should be noted that P_1(pitch) and P_2 (first elastic mode) attain their highest values close to the wave period of 18 s, at which period P_0(heave) is zero. The response of the structure in head waves of 11 and 18 s periods is shown in Figs. 11(a) and 11(b), respectively. The wave period of 18 s corresponds to a wavelength of approximately 500 m, which is equal to the total length of the structure made of five modules,

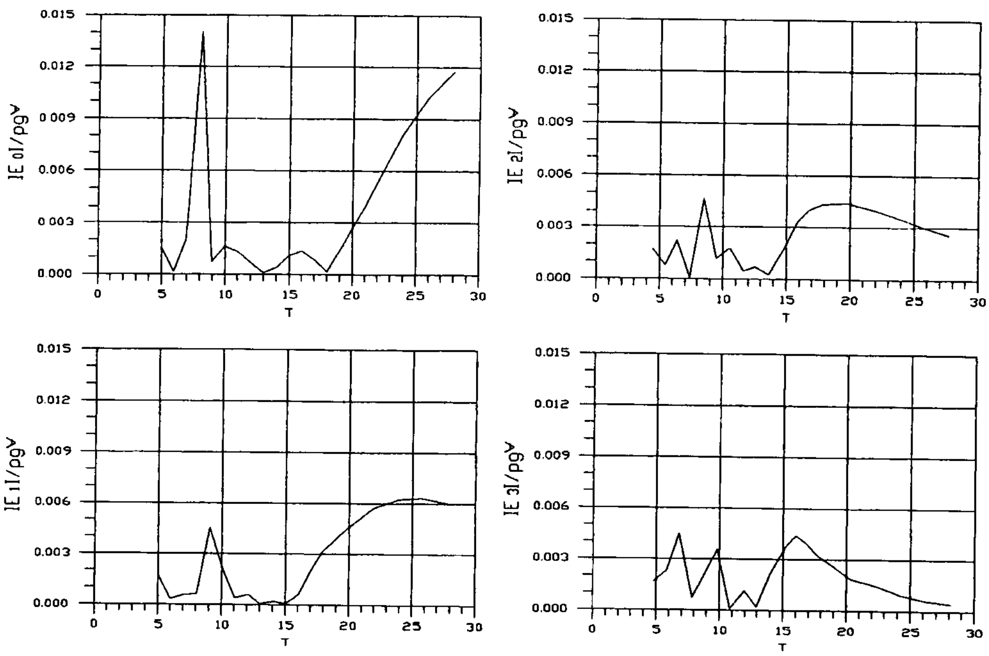

Fig. 9. Generalized wave exciting force $E_r/\rho\, gV$ for r=0, 1, 2, 3 in head seas.

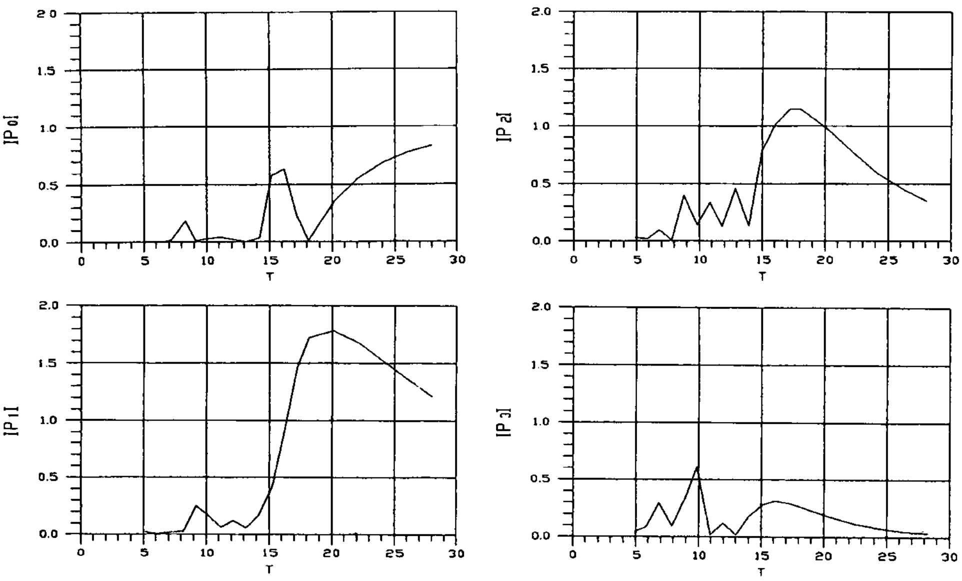

Fig. 10. Amplitudes of principal coordinates $|P_r|$ for r=0, 1, 2, 3 in head seas.

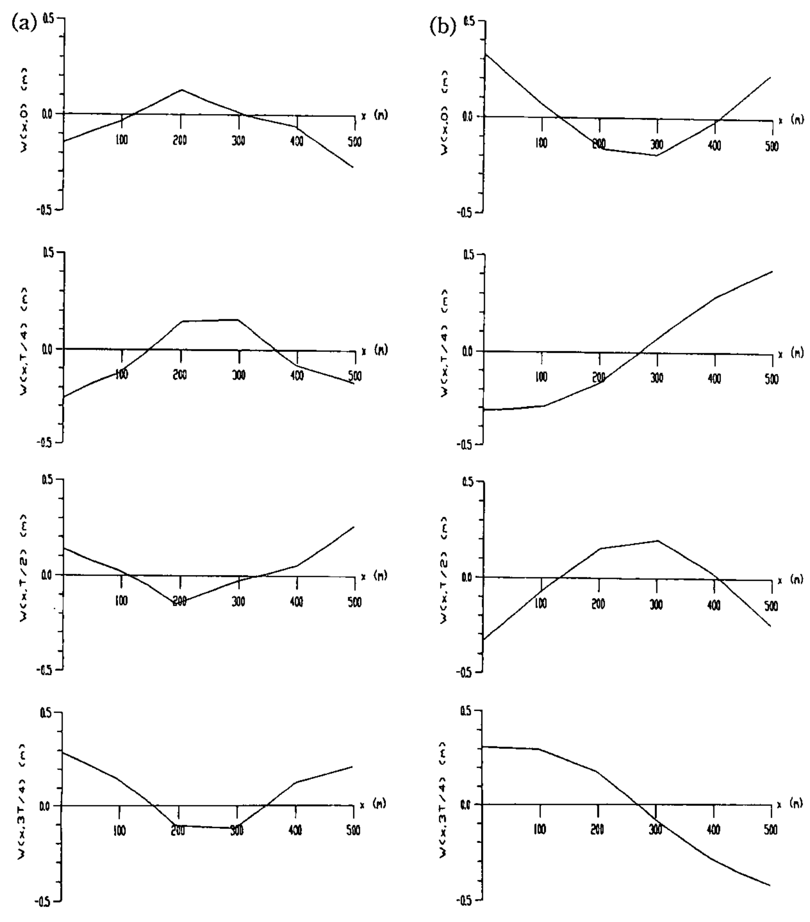

Fig. 11. Response at different wave phases; (a) wave period=11 s, wave length=189 m, (b) wave period=18 s, wave length=506 m.

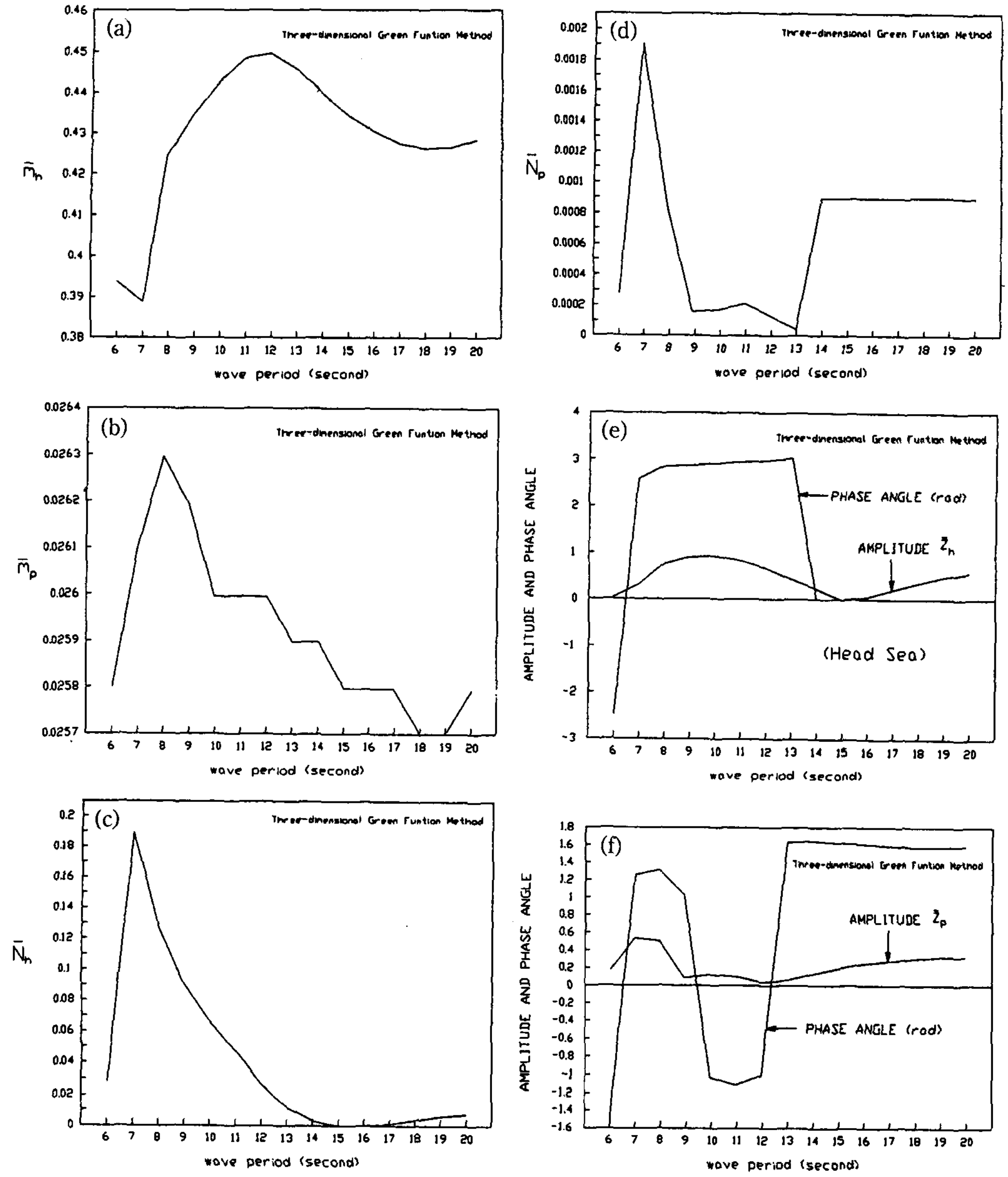

Fig. 12. Hydrodynamic properties; (a) Added mass (in heave), (b) Added moment of inertia (in pitch), (c) Hydrodynamic damping (in heave), (d) Hydrodynamic damping (in pitch), (e) Heave exciting force, (f) Pitch exciting moment.

while the wave period of 11 s corresponds to a wavelength of 190 m, which is about 2.5 times shorter than the length of the structure consisting of five modules.

From these results it is seen that because of the flexibility of the connectors, the first bending mode is likely to occur even though the stiffness of the individual modules is very high.

6.2 The Hinged Connector Model

The hydrodynamic coefficients and exciting forces are calculated by a three-dimensional GFM for a single module. In Figs. 12(a)~(e), the added-mass coefficients in heave and pitch are $\bar{m}_h = m_h/(\rho\forall)$ and $\bar{m}_p = m_p/(\rho\forall L^2)$, respectively; the damping coefficients in heave and pitch are $\bar{N}_h = N_h/(\rho\forall\sqrt{g/L})$ and $\bar{N}_p = N_p/(\rho\forall L^2\sqrt{g/L})$, respectively; and the heave force and

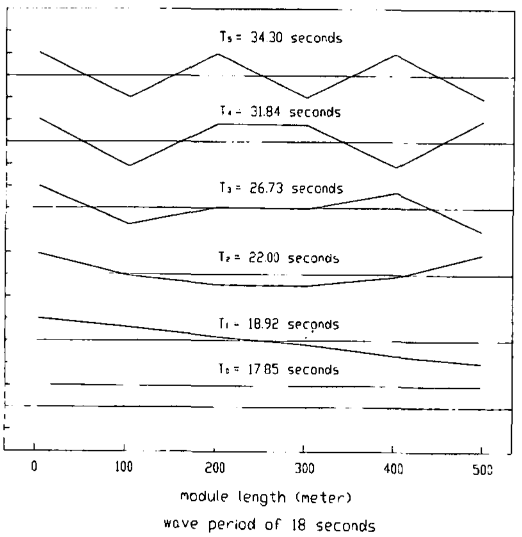

Fig. 13. Structural mode shape (wet).

pitch moment are $\bar{Z}_h = Z_h/(\rho g \forall (H/2)L)$ and $\bar{Z}_p = Z_p/(\rho g \forall H/2)$, respectively. The calculated natural periods and the mode shapes of the structure are shown in Fig. 13. In this figure T_j refers to the natural period of each mode. These results include the effect of added mass for a wave period of 18 s. It is shown from Fig. 13 that the modal shape of the shortest natural period corresponds to heave, and the modal shape of the longest natural period corresponds to pitch. By adjusting the connector stiffness in heave or pitch or both, the order of the modal shapes can be changed. It may be desirable to give the modal shape corresponding to heave the shortest natural period if the wave energy is concentrated at small periods. Obviously, one needs to know the statistics of irregular waves in order to make a judgment about the concentration of wave energy.

The responses of the structure to head seas at wave periods of 11 and 18 s, and of unit wave amplitude, have been calculated at t=0, T/4, T/2 and 3T/4, where T is, as usual, the wave period. These results are shown in Figs. 14(a) and 14(b).

A comparison of the results obtained in Sections 6.1 and 6.2 shows that, since the stiffness of connectors is much smaller than that of each module, the application of hinge connector may be more effective and also give acceptable results. This is especially

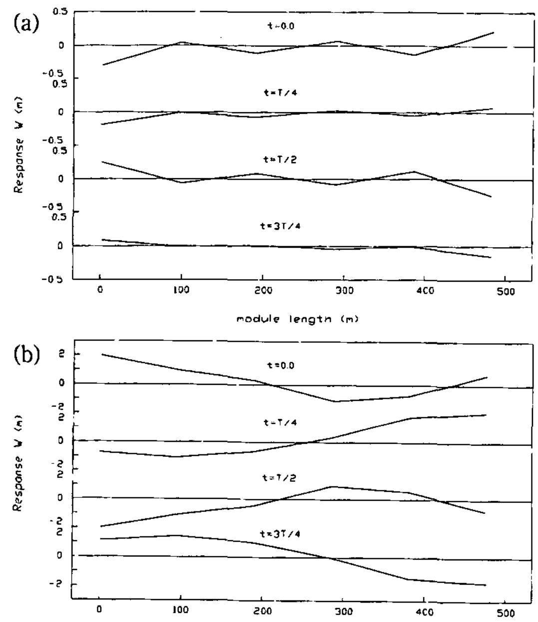

Fig. 14. Response of RMFC model; (a) wave length=189 m, wave period=11 s, (b) wave length=506 m, wave period=18 s.

true if the response is high, as at T=18 s. When the response level is low, as at T=11 s, the deflection shapes are not as close, but the amplitudes are in good agreement. It is also shown, perhaps surprisingly, that strip theory for the calculation of hydrodynamic coefficients offers as good results as the three-dimensional GFM.

7. CONCLUSIONS

Flexible body analysis has been given to a VLFS by applying the hydroelasticity theory. The analysis provides motions and section forces, which are useful for the analysis and design of VLFS. The numerical results are presented respectively for two types of module connector, and shown that while the hinge connectors result in greater motion, the rigid connectors increase substantially the sectional moments. The hinged connector modules also appears to be useful for the engineering design of a VLFS. Both the boundary-element method and Green function method give numerical results which are in reasonable mutual agreement.

REFERENCES

Andres, J.M., 1986. Nonlinear wave and current loading on large OTEC pipe, Ph.D. dissertation, Department of Ocean Engineering, University of Hawaii.

Bishop, R.E.D., and Price, W.G., 1979. *Hydroelasticity of ships*, Cambridge University Press, U.K.

Brebbia, C.A., 1978. *The boundary element method for engineering*, Pentech Press, London.

Flokstra, C., 1974. Comparison of ship motion theories with experiments for a container ship, *Int. Shipbldg. Prog.*, **21**: pp. 168-189.

Frank, W., 1967. Oscillation of cylinders in below the free surface of deep fluids, *NSRDC Report 2375*, Naval Ship R & D Center, Bethesda.

Garrison, C.J., 1984. Interaction of oblique waves with an infinite cylinder, *Applied Ocean Research*, **6**(1): pp. 4-15.

Gerritsma, J. and Beukelman, W., 1964. The distribution of the hydrodynamic force on a heaving and pitching ship model in still water, *5th Symp. on Naval Hydrodynamics*, pp. 219-251.

Hartz, B.J., 1981. Dynamic response of the Hood Canal floating bridge failure, *Proc. 3rd International Conf. on Structural Safety and Reliability*, Trondheim, pp. 545-557.

Heller, S.R. and Abramson, H.N., 1959. Hydroelasticity: A new naval science, *J. Am. Soc. Naval Engrs.*, **71**(2): pp. 205-209.

John, F., 1950. *On the motion of floating bodies II, Communications on pure and applied mathematics*, Vol. 3, Interscience Publishers, New York, pp. 45-101.

Kellog, O.D., 1929. *Foundations of potential theory*, Dover Publications, New York.

Lee, C.M., Jones, H. and Bedel, J.W., 1971. Added mass and damping coefficients of heaving twin cylinders in a free surface, *NSRDC Report 3695*, Naval Ship R & D Center, Bethesda.

Mei, C.C., 1989. *The applied dynamics of ocean surface waves*, World Scientific Publishing Co., 2nd ed.

Rayleigh, L., 1984. *The theory of sound*, 2nd ed., Art 94, Macmillan, London, 8.

Salvesen, N., Tuck, E.O., and Faltinsen, O., 1970. Ship motions and sea loads, *Trans. SNAME*, **78**, pp. 250-287.

Seidl, L., 1973. Theoretical investigations of optimization of the platform's seakeeping characteristics, *Univ. of Hawaii, Seagrant, Tech. Rep.* (2), May.

St. Denis, M., 1974. The winds, currents and waves at the suite of the Floating City off Waikiki, *Univ. of Hawaii, Seagrant-CR-75-01, Tech. Rep.* (1), Dec.

Timoshenko, S. P., Young, D. H. and Weaver, W., 1974. *Vibration problems in engineering*, 4th ed., Wiley, New York.

USD, 1990. Floating airport San Diego workshop, University of San Diego, San Diego, CA, Feb.

Wehausen, J.V. and Laitone, E.V., 1960. Surface waves, *Hundbuch der Physik, Band 9, Springer Verlag*, Berlin, pp. 446-776.